

SUPPORTING INFORMATION

Supporting Methods

Generation of stable cell lines

Cell lines that stably overexpress or knock down LRRK1 or LRRK2 were generated via lentiviral (LV) vector transduction. LV vectors were produced by the Leuven Viral Vector core as previously described (Geraerts et al., 2005; Civiero et al., 2012). For transduction in cell culture, 50 000 cells (HEK293T or SH-SY5Y) were plated in a 24-well plate and grown in DMEM with 8% (HEK293T) or 15% (SH-SY5Y) fetal bovine serum and for SH-SY5Y cells additionally with 100X MEM Non-Essential Amino Acids Solution (Life technologies). The next day, about 10^6 transducing units (TU) of vector were diluted into the cell supernatant and incubated for 1-3 days. When cells reached 80-100% confluence, cells were trypsinized and transferred to a 6-well plate. In case a selection marker was co-expressed, cells were further cultured with normal culture medium containing selection antibiotics (blasticidin selection was performed with 10 μ g/ml of blasticidin, hygromycin selection with 250 μ g/ml hygromycin). Cells were then further expanded for use in the experiments. For cells transduced with 2 different LV vectors, such as cells transduced with a short hairpin construct as well as a LRRK1 or LRRK2 overexpression construct, transductions were performed serially.

Metabolic labeling

Metabolic labeling was performed as described by Taymans *et al.* (Taymans et al., 2013). Cells expressing LRRK1 or LRRK2 were rinsed two times in DMEM without

phosphates and then metabolically labeled with 5 $\mu\text{Ci}/\text{cm}^2$ orthophosphate- P^{32} (Perkin-Elmer, Waltham, MA, USA) in DMEM without phosphates at 37°C. Following 4-8 hours labeling, cells were lysed and LRRK1 or LRRK2 proteins were immunoprecipitated using anti-Flag M2 agarose beads. In experiments with compound treatment, a compound treatment step was included between labeling and lysis in which compound or solvent were diluted into the labeling medium at the desired concentration and for the desired contact time. Immunoprecipitated proteins were resolved on 3-8% tris acetate SDS-PAGE gels and blotted to PVDF membranes. Incorporated P^{32} was detected by autoradiography using a Storm 840 phosphorescence scanner (GE Healthcare). The same membranes were stained with Ponceau S (Sigma, St. Louis, MO, USA) to correct for protein loading and probed with anti-Flag antibody to confirm the presence of LRRK1 or LRRK2. Densitometric analysis of the bands on the blot autoradiograms and immunoreactivity were performed using Aida analyzer v1.0 (Raytest, Straubenhardt, Germany) or ImageJ software (NIH, USA). Levels of phosphorylation incorporation were calculated as the ratio of the autoradiographic signal over the immunoreactivity level and normalized to levels of the control sample. All conditions were tested in triplicate.

Immunocytochemistry

For immunocytochemistry, cells were plated out and grown on 12 mm coverslips in a 24-well plate or in 8-well chamber slides. After washing with PBS, cells were fixed with 4% formaldehyde, 1xPBS for 15 min, followed by 2 wash steps with PBS. After permeabilization for 5 min with PBS + 0,1% Triton X-100, a 30 min blocking step with 10% goat serum (Dako cytomation, Glostrup, Denmark) in PBS was performed. This was followed by 2 h incubation with primary antibody(ies) in PBS. After three

washes with PBS for 5 min, cells were incubated for 1 h with appropriate secondary antibody(ies) (Alexa Fluor 488 or Alexa Fluor 555- conjugated anti IgG antibody, 1/500, Molecular Probes, Invitrogen) and again 3 times washed for 5 min with PBS. The coverslips were mounted on a microscope slide with Mowiol (Sigma) supplemented with DAPI (4',6-diamidino-2-phenylindole, Roche) to visualize nuclei. Visualization was performed by confocal laser scanning microscopy (Fluoview 1000, Olympus, Shinjuku, Tokyo, Japan).

Phosphosite analysis by mass spectrometry

Phosphosite mapping was performed on purified Flag-tagged LRRK1 and LRRK2. In brief, cells expressing 3xFlag-LRRK1 or 3xFlag-LRRK2 were solubilized in buffer (20 mM Tris-HCl pH 7.5, 150 mM NaCl, 1 mM EDTA, 0.5% Tween 20 or 1% Triton X-100, 2.5 mM sodium pyrophosphate, 1mM beta-glycerophosphate, 1 mM NaVO₄, protease inhibitor mixture) and lysates were centrifuged for 30 minutes at 14000xg. Afterwards, lysates containing 3xFlag-tagged protein were incubated with anti-Flag M2 agarose beads for 2 hours at 4°C on a rotator. After extensive washings of the affinity beads, proteins were eluted using SDS sample buffer and were separated by SDS-PAGE. The protein band of interest was excised and subjected to an overnight digestion at 37°C with 250 ng trypsin in 200 mM ammonium bicarbonate. The resulting peptide mixture was either analyzed by nano LC-MS/MS on a 4000 QTRAP mass spectrometer (AB SCIEX, Framingham, MA, USA) or subjected to phosphopeptide enrichment as described in Venerando A. *et al.* (Venerando et al., 2013) and analyzed by nano LC-MS/MS on a LTQ-Orbitrap XL (Thermo Fisher Scientific). In the latter case, the sample was loaded into a 10 cm pico-frit column (75µm internal diameter, 15 µm tip, New Objectives) packed in house with C18

material (Aeris Peptide 3.6 μm XB-C18, Phenomenex) and peptides were separated using a linear gradient of acetonitrile/0.1% formic acid from 3% to 40% in 20 min on a nano HPLC Ultimate 3000 system (Dionex – Thermo Fisher Scientific). In the former case, nano LC was performed on a PepMap C18 column developed with a linear gradient of acetonitrile/0.1% formic acid from 6% to 40% in 30 min on a similar capillary liquid chromatography system (Thermo Fisher Scientific).

In the 4000QTRAP approach, putative phosphorylated peptides were pinpointed by precursor 79 (-) ion scanning in a first LC-MS run, while in a second LC-MS run, MRM (multiple reaction monitoring) - induced product (+) ion scanning was executed to determine peptide sequences and to localize phosphorylated residues. In the LTQ-Orbitrap XL approach, the instrument was operated in a data dependent mode: a full MS scan in the Orbitrap (60000 resolution) was followed by a neutral loss-triggered dependent acquisition in the linear trap on the 3 most intense ions. The same sample was analyzed again using the same chromatographic conditions but with a multi-stage activation protocol for MS analysis. Acquired spectra were analyzed with the software Proteome Discoverer 1.4 (Thermo Fisher Scientific) interfaced with a Mascot Search engine version 2.2.4 (Matrix Science) using the human session of the Uniprot database (version 20121120). For database searching, trypsin was set as enzyme with up to 1 missed cleavage. Carboxymethyl cysteine was set as fixed modification, while methionine oxidation and phosphorylation of Ser, Thr, and Tyr were set as variable modifications. Precursor and fragment tolerance were set to 10 ppm and 0.6 Da, respectively. The software performed also a search against a randomized database, and data were filtered to keep only spectra with a False Discovery Rate (FDR) of 5% or less. In the 4000 QTRAP approach, acquired spectra were subjected to MASCOT search engine version 2.2.2 using a custom database

containing LRRK1 and LRRK2 sequences. In both approaches, spectra relative to phosphopeptides were manually inspected to confirm the identity of the peptides and the correct assignment of the phosphorylation sites.

Supporting Figures

Figure S1. LRRK1 and LRRK2 cellular phosphorylation sites map to distinct protein regions. LRRK1 and LRRK2 proteins isolated from HEK293T cells were submitted to proteolytic cleavage and phosphosites were identified by ESI-MS/MS. (A) Coomassie brilliant blue staining of SDS-PAGE gel with purified LRRK1 and LRRK2 proteins used in phosphosite analysis. (B) Alignment of LRRK1 and LRRK2 domain structure as well as alignment of sequences around LRRK1 or LRRK2 phosphosites (those LRRK2 phosphosites identified in the present study are indicated with an asterisk, while previously reported phosphosites are also given). (C) Annotated MS/MS spectra of phosphopeptides in LRRK1 and LRRK2.

Figure S2: Visualization of LRRK1 and LRRK2 subcellular localization following stimulation by rhodamine labeled epidermal growth factor. EGF induced translocation of LRRK1 or LRRK2 to endosomes was assessed in 4 different SH-SY5Y cell lines. (A) SH-SY5Y cells with stable overexpression of eGFP-LRRK1 and expression of a control knockdown construct for genetic depletion (ctrl miR). (B) SH-SY5Y cells with stable overexpression of eGFP-LRRK2 and expression of a control knockdown construct for genetic depletion. (C) SH-SY5Y cells with stable overexpression of eGFP-LRRK1 and depletion of endogenous LRRK2 (LV_miR_LRRK2_6251). (D) SH-SY5Y cells with stable overexpression of eGFP-LRRK2 and depletion of endogenous LRRK1 (LV_miR_LRRK1_6734). Cell lines were treated with EGF-rhodamine (EGF-Rh, 100 ng/ml) and endosomal EGF-Rh was imaged together with eGFP-LRRK1 or eGFP-LRRK2 at the indicated time points (0, 5, 15 and 30 minutes after addition of EGF-Rh) as described in materials and methods.

Quantifications of the % of cells showing translocation of LRRK1 or LRRK2 to EGF-Rh-positive endosomes is given in Figure 4. Scale bar, 10 μ m applies to all photomicrographs.

Figure S3: EGF induced translocation of LRRK1 in control cell lines and in cells with genetic depletion of LRRK2. Cell lines were treated with EGF (100 ng/ml) and eGFP-LRRK1 was imaged at the indicated time points (0, 5, 15 and 30 minutes after addition of EGF-Rh) as described in materials and methods. Representative confocal microscopy images are given in (A) of eGFP-LRRK1 30 minutes after EGF or solvent treatment, both for the control cell lines (BsdR ctrl, rows 1 and 2 of images) as well as for the knockdown cell lines: eGFP-LRRK1 with LRRK2 knockdown (construct LV_miR_LRRK2_6251, rows 3 and 4 of images). (B) The % of cells displaying an endosome-like subcellular localization of eGFP-LRRK1 (minimum 5 endosome-like accumulations of eGFP-LRRK1 per cell) were determined by manual scoring. Quantifications are given for eGFP-LRRK1 cell lines expressing control for knockdown constructs (BsdR ctrl and miR ctrl) or LRRK2 knockdown constructs (LRRK2 KD1, KD2 and KD3 corresponding to constructs LV_miR_LRRK2_2384, LV_miR_LRRK2_6251, LV_miR_LRRK2_7814). Scale bar, 10 μ m applies to all photomicrographs.

Figure S4: Co-localisation of EGF-stimulated eGFP-LRRK1 with endosomes

EGF-stimulated eGFP-LRRK1-positive structures are endosomal as shown by co-staining with the endosomal marker EEA1. Shown here are confocal microscopy images of DAPI (blue), eGFP-LRRK1 (green) and EEA1 (red) of SH-SY5Y cells with stable expression of eGFP-LRRK1 15 minutes after stimulation with EGF (100

ng/ml). In the overlay image (panel 4) co-staining is observed of eGFP-LRRK1 and EEA1 (arrows). Scale bar, 10 μ m.

Description of raw data tables

Three text files are included that detail the output from Protoarray Prospector. In the first two files 3xFlag-LRRK1 and -LRRK2 are compared to 3Flag-eGFP, in the third file 3xFlag-LRRK1 and 3xFlag-LRRK2 are compared.

Supporting Tables

Supporting Table 1 : List of interacting proteins identified via protein microarray

A. Specific for LRRK1

NCBI accession number	Description	GFP	LRRK1	LRRK2
NM_004873.1	BCL2-associated athanogene 5 (BAG5), transcript variant 2	0.58	15.55	0.46
NM_016404.1	hypothetical protein HSPC152 (HSPC152)	-0.01	13.91	-0.52
NM_005228.3	epidermal growth factor receptor (erythroblastic leukemia viral (v-erb-b) oncogene homolog, avian) (EGFR)	-0.31	13.21	-0.28
NM_004281.2	BCL2-associated athanogene 3 (BAG3)	1.36	13.08	1.46
NM_001015048.2	BCL2-associated athanogene 5 (BAG5)	1.19	11.62	0.91
NM_005228.3	epidermal growth factor receptor (erythroblastic leukemia viral (v-erb-b) oncogene homolog, avian) (EGFR)	-0.31	8.71	-0.25
NM_019590.4	KIAA1217 (KIAA1217)	2.35	7.78	0.38
NM_004323.5	BCL2-associated athanogene (BAG1)	1.03	7.61	1.53
NM_002020.4	fms-related tyrosine kinase 4 (FLT4), transcript variant 2	0.14	7.40	0.64
NM_004282.2	BCL2-associated athanogene 2 (BAG2)	-0.28	7.21	1.01
NM_005861.2	STIP1 homology and U box-containing protein 1	-0.12	6.90	0.17
NM_020526.3	Ephrin receptor A8 (EPHA8), transcript variant 2	2.21	6.48	0.34
NM_020975.4	ret proto-oncogene (RET), transcript variant 4	-0.55	5.87	0.03
NM_170662.3	Cas-Br-M (murine) ecotropic retroviral transforming sequence b (CBLB)	0.31	5.08	0.60
NM_144777.2	sciellin (SCEL)	1.91	4.79	2.94

NM_052887.2	toll-interleukin 1 receptor (TIR) domain containing adaptor protein (TIRAP), transcript variant 1	2.82	4.76	-0.11
NM_033421.2	sorting nexin family member 21 (SNX21), transcript variant 1	2.74	3.98	1.47
XM_005266343.1	cytoskeleton associated protein 2 (CKAP2)	2.72	3.61	0.49
NM_015532.2	glutamate receptor, ionotropic, N-methyl D-aspartate-like 1A (GRINL1A), transcript variant 1	0.20	3.53	0.22
NM_201280.1	muted homolog (mouse) (MUTED)	1.56	3.51	1.94
NM_022976.1	fibroblast growth factor receptor 2 (bacteria-expressed kinase, keratinocyte growth factor receptor, craniofacial dysostosis 1, Crouzon syndrome, Pfeiffer syndrome, Jackson-Weiss syndrome) (FGFR2), transcript variant 1	0.56	3.41	0.55
NM_153435.1	outer dense fiber of sperm tails 2 (ODF2)	2.75	3.40	2.24
NM_005157.4	v-abl Abelson murine leukemia viral oncogene homolog 1 (ABL1), transcript variant a	2.84	3.33	2.76
NM_032682.5	forkhead box P1 (FOXP1)	0.07	3.27	1.49
NM_002073.2	guanine nucleotide binding protein (G protein), alpha z polypeptide (GNAZ)	2.09	3.14	1.26
NM_024695.1	lectin, mannose-binding, 1 like (LMAN1L)	1.71	3.12	1.60
NM_173519.1	retinaldehyde binding protein 1-like 1 (RLBP1L1)	0.88	3.10	0.74
NM_031483.3	E3 ubiquitin-protein ligase Itchy homolog	1.57	3.07	2.31
NM_032349.1	nudix (nucleoside diphosphate linked moiety X)-type motif 16-like 1 (NUDT16L1)	1.55	3.03	0.90
NM_014667.1	vestigial like 4 (Drosophila) (VGLL4)	1.40	3.02	1.20

B. Specific for LRRK2

NCBI Reference sequence	Description	GFP	LRRK1	LRRK2
NM_145690.2	14-3-3 protein zeta/delta	0.50	-0.12	5.27
NM_003404.2	tyrosine 3-monooxygenase/tryptophan 5-monooxygenase activation protein, beta polypeptide (YWHAB), transcript variant 1	1.72	2.12	4.70
NM_024885.3	Transcription initiation factor TFIID subunit 7-like	1.54	0.50	4.22
NM_004449.3	v-ets erythroblastosis virus E26 oncogene homolog (avian) (ERG), transcript variant 2	2.82	2.65	4.15
XM_374177.2	PREDICTED: Homo sapiens hypothetical LOC389415 (LOC389415)	1.50	1.42	4.13
NM_018230.2	nucleoporin 133kDa (NUP133)	2.84	2.52	3.99
NM_018686.4	cytidine monophosphate N-acetylneuraminic acid synthetase (CMAS)	2.40	1.74	3.97
NM_017980.4	LIM and senescent cell antigen-like domains 2 (LIMS2)	1.59	1.50	3.91
NM_003160.1	Serine/threonine-protein kinase 13	1.78	1.95	3.87
NM_002922.2	regulator of G-protein signaling 1 (RGS1)	1.90	2.87	3.85
NM_016212.1	TP53TG3 protein (TP53TG3)	2.50	0.73	3.79
NM_001387.2	Dihydropyrimidinase-related protein 3	2.13	2.73	3.75
NM_006387.5	calcium homeostasis endoplasmic reticulum protein (CHERP)	2.76	1.00	3.69
NM_018140.3	centrosomal protein 72kDa (CEP72)	1.50	2.39	3.66
NM_032345.1	within bgcn homolog (Drosophila) (WIBG)	1.77	2.35	3.61
NM_030906.3	serine/threonine kinase 33 (STK33)	2.90	1.05	3.54
NM_203291.1	retinoblastoma binding protein 8 (RBBP8)	1.71	0.93	3.54
XM_001133281.1	PREDICTED: Homo sapiens hypothetical protein LOC283663 (LOC283663), mRNA	1.89	1.73	3.51
NM_007177.1	Protein FAM107A	1.97	1.66	3.50
NM_152736.2	Zinc finger protein 187	1.34	0.94	3.49

NM_022491.2	Sin3 histone deacetylase corepressor complex component SDS3	-0.20	0.04	3.43
NM_003113.3	SP100 nuclear antigen (SP100)	1.90	1.67	3.42
NM_013242.1	chromosome 16 open reading frame 80 (C16orf80)	2.83	2.05	3.41
NM_145865.1	ankyrin repeat and sterile alpha motif domain containing 4B (ANKS4B)	2.93	1.90	3.39
NM_005158.4	Tyrosine-protein kinase ABL2	1.63	0.91	3.39
NM_201567.1	cell division cycle 25 homolog A (S. pombe) (CDC25A), transcript variant 2	0.82	0.54	3.38
NM_001626.2	v-akt murine thymoma viral oncogene homolog 2 (AKT2)	2.72	1.85	3.37
NM_032728.2	phosphatidic acid phosphatase type 2 domain containing 3 (PPAPDC3)	2.18	1.67	3.35
NM_152266.1	chromosome 19 open reading frame 40 (C19orf40)	1.71	2.56	3.34
NM_005517.2	high-mobility group nucleosomal binding domain 2 (HMGN2)	1.38	1.22	3.33
BC011916.1	chromosome 10 open reading frame 65 (C10orf65)	2.49	2.45	3.32
NM_022347.1	interferon responsive gene 15 (IFRG15)	2.23	1.11	3.31
NM_024546.2	RING finger protein 219	1.55	0.70	3.28
NM_003720.1	Proteasome assembly chaperone 1	0.78	1.70	3.28
NM_031465.2	chromosome 12 open reading frame 32 (C12orf32)	1.84	1.75	3.27
NM_017856.1	gem (nuclear organelle) associated protein 8 (GEMIN8), transcript variant 3	0.60	1.76	3.27
NM_030575.1	hypothetical protein MGC10334 (MGC10334)	1.88	0.18	3.25
NM_001284280.1	Serine/threonine-protein phosphatase 4 regulatory subunit 3A	1.45	1.23	3.24
BC050563.1	hypothetical protein LOC202051 (LOC202051)	2.44	1.80	3.23
NM_199054.1	MAP kinase interacting serine/threonine kinase 2 (MKNK2), transcript variant 2	1.87	1.36	3.22
NM_003318.4	TTK protein kinase (TTK)	2.91	2.28	3.20
NM_001010844.1	Interleukin-1 receptor-associated kinase 1-binding protein 1	1.23	1.79	3.20
NM_022772.2	EPS8-like 2 (EPS8L2)	1.26	0.94	3.20
NM_001023.2	ribosomal protein S20 (RPS20)	1.27	0.91	3.18
NM_015534.4	zinc finger, ZZ-type containing 3 (ZZZ3)	2.33	2.02	3.18

NM_001004285.1	DNA fragmentation factor, 40kDa, beta polypeptide (caspase-activated DNase) (DFFB), transcript variant 3	1.26	1.43	3.15
NM_021643.3	Tribbles homolog 2	2.34	1.02	3.12
NM_175923.2	hypothetical protein MGC42630 (MGC42630)	2.15	2.45	3.11
NM_001018061.1	UPF0544 protein C5orf45 [Source:UniProtKB/Swiss-Prot;Acc:Q6NTE8]	1.28	0.34	3.11
NM_018230.2	Nuclear pore complex protein Nup133	2.13	2.20	3.11
NM_004454.1	ets variant gene 5 (ets-related molecule) (ETV5)	0.94	1.03	3.10
NM_005544.2	insulin receptor substrate 1 (IRS1)	1.86	1.96	3.05
NM_175571.2	GTPase, IMAP family member 8 (GIMAP8)	-0.32	-0.56	3.04
NM_017544.3	NF-kappaB repressing factor (NKRF)	0.81	0.78	3.03
NM_006231.3	polymerase (DNA directed), epsilon (POLE)	1.59	1.30	3.02
NM_014395.2	dual adaptor of phosphotyrosine and 3-phosphoinositides (DAPP1)	2.18	2.52	3.01
BC028935.1	chromosome 3 open reading frame 64 (C3orf64)	2.18	2.28	3.00

C. Common interactors

NCBI	Description	GFP	LRRK1	LRRK2
NM_005255	cyclin G associated kinase (GAK)	2.52	9.67	5.81
NM_001819.1	chromogranin B (secretogranin 1) (CHGB)	2.19	7.90	7.32
NM_139355	megakaryocyte-associated tyrosine kinase (MATK), transcript variant 2	2.84	5.89	3.23
NM_012224	NIMA (never in mitosis gene a)-related kinase 1 (NEK1)	2.78	5.14	4.65
NM_016224.3	Sorting nexin-9	1.48	4.53	4.87
NM_006449.2	CDC42 effector protein (Rho GTPase binding) 3 (CDC42EP3)	2.13	4.06	5.30
NM_002989	C-C motif chemokine 21	0.39	3.88	3.38
NM_005157.4	v-abl Abelson murine leukemia viral oncogene homolog 1 (ABL1), transcript variant a	1.59	3.63	3.10
NM_178552	chromosome 22 open reading frame 33 (C22orf33)	2.56	3.57	3.56
NM_016403	CWC15 homolog (S. cerevisiae) (HSPC148)	2.03	3.56	3.53
NM_020168.3	p21 protein (Cdc42/Rac)-activated kinase 6 (PAK6)	2.20	3.43	3.93
NM_004092.2	Enoyl-CoA hydratase, mitochondrial	1.52	3.41	4.13
NM_021639.2	GC-rich promoter binding protein 1-like 1 (GPBP1L1)	1.77	3.27	4.30
NM_006110.1	CD2 (cytoplasmic tail) binding protein 2 (CD2BP2)	2.05	3.15	3.01
NM_014456	programmed cell death 4 (neoplastic transformation inhibitor) (PDCD4)	2.43	3.12	3.59
NM_014972.1	Transcription factor 25	0.79	3.06	4.12

Supporting Table 2 : List of interacting proteins identified with AP-MS approach

A. Specific for LRRK1

	NCBI accession number	Description	N° of unique peptides	Sequence coverage	Protein probability score	Remarks
1	NM_024652	Leucine-rich repeat kinase 1 (LRRK1)	25	17,00%	100,00%	
2	NM_003127	spectrin, alpha, non-erythrocytic 1 (SPTAN1)	19	15,00%	100,00%	
3	NM_003128	spectrin, beta, non-erythrocytic 1 (SPTBN1)	9	6,60%	100,00%	
4	NM_002086	Growth factor receptor-bound protein 2 (GRB2)	4	34,00%	100,00%	
5	NM_004924	actinin, alpha 4 (ACTN4)	5	9,00%	100,00%	
6	NM_080881	Drebrin 1 (DBN1)	4	10,00%	100,00%	
7	NM_183001	SHC (Src homology 2 domain containing) transforming protein 1 (SHC1)	4	12,00%	100,00%	
8	NM_012223	Myosin-Ib (MYO1B)	2	3,50%	100,00%	
9	NM_001003	ribosomal protein, large, P1 (RPLP1)	2	29,00%	100,00%	
10	NM_006088	tubulin, beta 4B class Ivb (TUBB4B)	2	27,00%	100,00%	
11	NM_012223	Myosin-Ib (MYO1B)	2	1,80%	100,00%	Also identified with low score in one of the two control replicates

B. Specific for LRRK2

	NCBI accession number	Description	Number of unique peptides	Sequence coverage	Protein probability score	Remarks
1	NM_001417	Eukaryotic translation initiation factor 4B (EIF4B)	3	11,00%	100,00%	
2	NM_006717	Spindlin-1 (SPIN1)	2	16,00%	100,00%	
3	NM_001293	chloride channel, nucleotide-sensitive, 1A (CLNS1A)	3	24,00%	100,00%	
4	NM_002295	ribosomal protein SA (RPSA)	2	9,50%	100,00%	
5	NM_006761	14-3-3 protein epsilon (YWHAE)	1	11,00%	92,00%	
6	NM_012479	14-3-3 protein gamma (YWHAG)	1	12,00%	92,00%	
7	NM_006826	14-3-3 protein theta (YWHAQ)	1	12,00%	92,00%	
8	NM_007002	adhesion regulating molecule 1 (ADRM1)	1	4,00%	92,00%	
9	NM_032378	Elongation factor 1-delta (EEF1D)	1	8,50%	92,00%	
10	NM_003758	Eukaryotic translation initiation factor 3 subunit J (EIF3J)	1	5,00%	92,00%	
11	NM_005348	heat shock protein 90kDa alpha (cytosolic), class A member 1 (HSP90AA1)	1	3,70%	92,00%	
12	NM_002767	Phosphoribosyl pyrophosphate synthase-associated protein 2 (PRPSAP2)	1	4,60%	92,00%	
13	NM_032311	polymerase (DNA-directed), delta interacting protein 3 (POLDIP3)	1	3,10%	92,00%	
14	NM_017659	Glutaminy-peptide cyclotransferase-like protein (QPCTL)	1	2,90%	92,00%	
15	NM_001018	40S ribosomal protein S15 (RPS15)	1	15,00%	92,00%	

C. Common interactors

	NCBI accession number	Description	Number of unique peptides	Sequence coverage	Protein probability score	Remarks
1	NM_003378	Neurosecretory protein VGF	LRRK1: 7 LRRK2: 1	LRRK1: 19% LRRK2: 3,1%	LRRK1: 100%; RRK2:87%	
2	NM_007355	heat shock protein 90kDa alpha (cytosolic), class B member 1 (HSP90AB1)	LRRK1: 2 LRRK2: 1	LRRK1: 6,6% LRRK2: 3,7%	LRRK1: 100% LRRK2: 92%	
3	NM_178014	tubulin, beta class I (TUBB)	LRRK1: 11 LRRK2: 3	LRRK1: 40% LRRK2: 9%	LRRK1: 100% LRRK2: 100%	
4	NM_006082	Tubulin alpha-1B (TUBA1B)	LRRK1: 5 LRRK2: 2	LRRK1: 20% LRRK2: 7,8%	LRRK1: 100% LRRK2: 100%	Also identified in one of the two control replicates
5	NM_006597	heat shock 70kDa protein 8 (HSPA8)	LRRK1: 3, LRRK2: 1	LRRK1: 8,7% LRRK2: 2,3%	LRRK1: 100% LRRK2: 92%	Also identified in one of the two control replicates

Supporting Table 3: List of primers used to generate lentiviral vectors expressing microRNA-based short hairpin RNA sequences.

Name of oligonucleotide	Oligonucleotide sequence	Start position of the short hairpin sequence in target's reference sequence
sh1 miR30 LRRK1 S	GAGCG GCCCAGGTCTCAGATGGAATTA <i>TAGTGAAGCCACAGATGTA</i> TAATTCATCTGAGACCTGGGG T	6734
sh1 miR30 LRRK1 AS	AGGCA CCCCAGGTCTCAGATGGAATTA <i>TACATCTGTGGCTTCACTA</i> TAATTCATCTGAGACCTGGGC C	
sh2 miR30 LRRK1 S	GAGCG TCGCCAGAGATTCTTCCTTTAT <i>TAGTGAAGCCACAGATGTA</i> ATAAAGGAAGAATCTCTGGCGT T	4366
sh2 miR30 LRRK1 AS	AGGCA ACGCCAGAGATTCTTCCTTTAT <i>TACATCTGTGGCTTCACTA</i> ATAAAGGAAGAATCTCTGGCGA C	
sh3 miR30 LRRK1 S	GAGCG CCAACACCATTTCAGAGGGTAT <i>TAGTGAAGCCACAGATGTA</i> ATACCCTCTGAATGGTGTGGC T	3351
sh3 miR30 LRRK1 AS	AGGCA GCAACACCATTTCAGAGGGTAT <i>TACATCTGTGGCTTCACTA</i> ATACCCTCTGAATGGTGTGGG C	
sh4 miR30 LRRK1 S	GAGCG CCGGTGGAGATGTTATCGTCAT <i>TAGTGAAGCCACAGATGTA</i> ATGACGATAACATCTCCACCGC T	6091
sh4 miR30 LRRK1 AS	AGGCA GCGGTGGAGATGTTATCGTCAT <i>TACATCTGTGGCTTCACTA</i> ATGACGATAACATCTCCACCGG C	
sh1 miR30 LRRK2 S	GAGCG ACGTGTGTATGAAGGAATGTTA <i>TAGTGAAGCCACAGATGTA</i> TAACATTCCTTCATACACACGA T	7814
sh1 miR30 LRRK2 AS	AGGCA TCGTGTGTATGAAGGAATGTTA <i>TACATCTGTGGCTTCACTA</i> TAACATTCCTTCATACACACGT C	

sh3 miR30 LRRK2 S	GAGCG AGCCAGAGGAAATGTCATTAT <i>TAGTGAAGCCACAGATGTA</i> ATAAATGACATTTCTCTGGCA T	6251
sh3 miR30 LRRK2 AS	AGGCA TGCCAGAGGAAATGTCATTAT <i>TACATCTGTGGCTTCACTA</i> ATAAATGACATTTCTCTGGCT C	
sh5 miR30 LRRK2 S	GAGCG ACCCAAATTGGTGGAACTCTTA <i>TAGTGAAGCCACAGATGTA</i> TAAGAGTTCCACCAATTTGGGA T	2384
sh5 miR30 LRRK2 AS	AGGCA TCCCAAATTGGTGGAACTCTTA <i>TACATCTGTGGCTTCACTA</i> TAAGAGTTCCACCAATTTGGGT C	

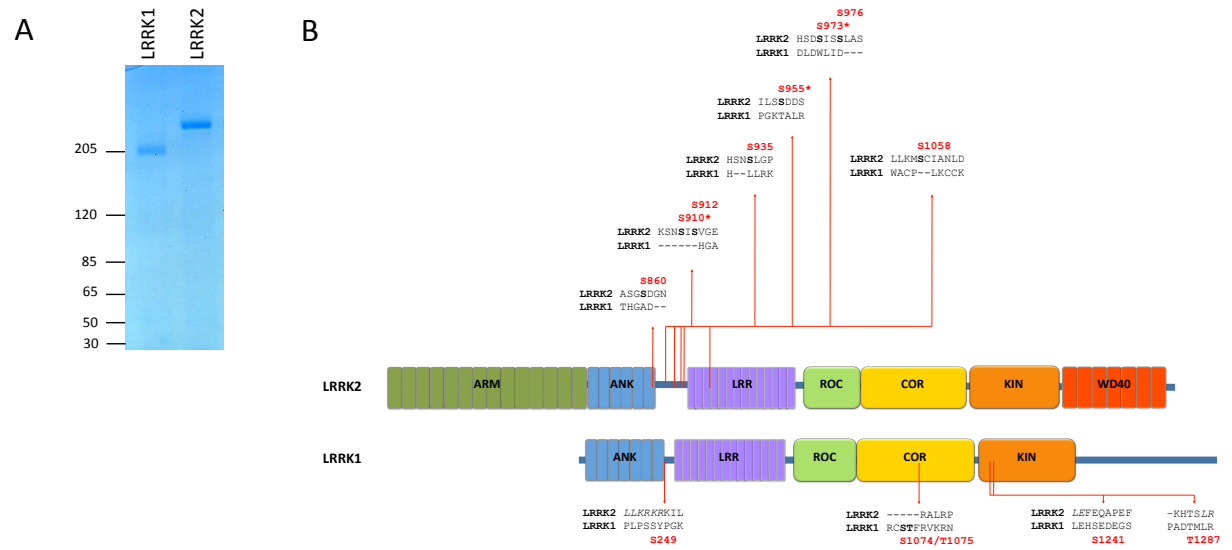
Table S3: List of primers used to generate lentiviral vectors expressing microRNA-based short hairpin RNA sequences. Sense and antisense primers are given, sequences depicted in bold correspond to the hairpin stem sequence containing the LRRK1 or LRRK2 target sequence, sequences given in italics are the loop sequence.

References

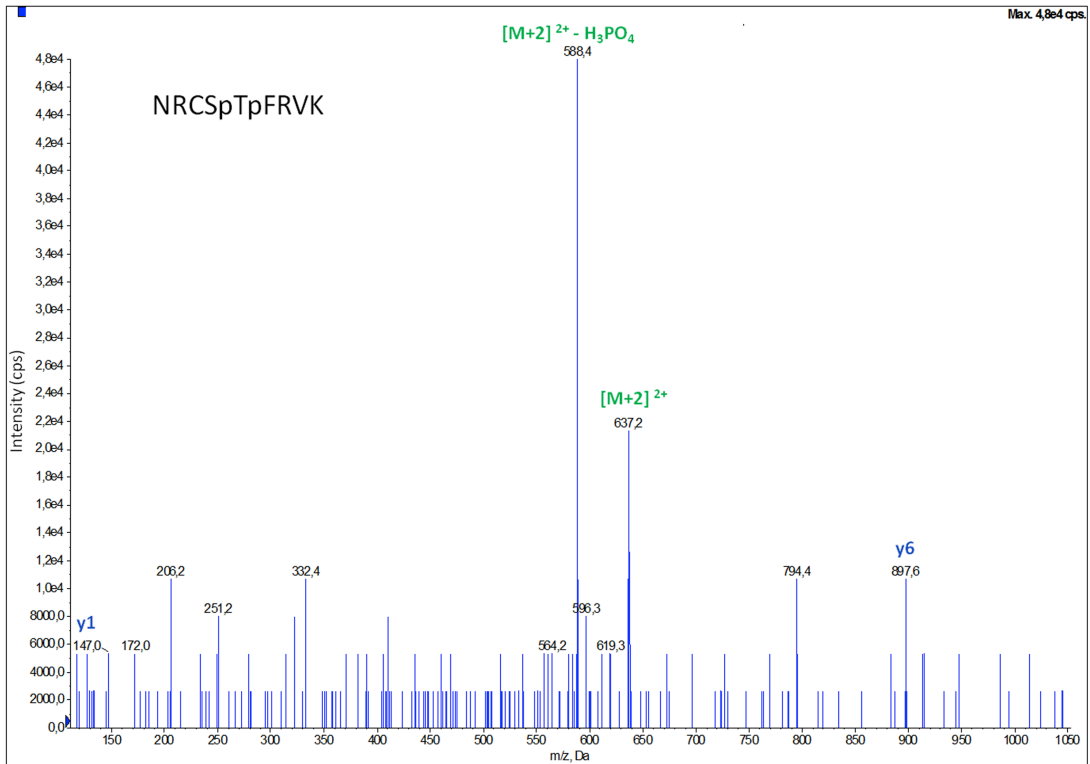
- Civiero, L., Vancaenenbroeck, R., Belluzzi, E., Beilina, A., Lobbestael, E., Reyniers, L., Fangye, G., Micetic, I., De Maeyer, M., Bubacco, L., Baekelandt, V., Cookson, M.R., Greggio, E., Taymans, J.-M., 2012. Biochemical characterization of highly purified leucine-rich repeat kinases 1 and 2 demonstrates formation of homodimers. *PLoS ONE* 7, e43472.
- Geraerts, M., Michiels, M., Baekelandt, V., 2005. Upscaling of lentiviral vector production by tangential flow filtration. *The journal of gene medicine*.
- Taymans, J.-M., Fangye, G., Baekelandt, V., 2013. Metabolic Labeling of Leucine Rich Repeat Kinases 1 and 2 with Radioactive Phosphate. *Journal of Visualized Experiments (JoVE)*.
- Venerando, A., Franchin, C., Cant, N., Cozza, G., Pagano, M.A., Tosoni, K., Al-Zahrani, A., Arrigoni, G., Ford, R.C., Mehta, A., Pinna, L.A., 2013. Detection of phospho-sites generated by protein kinase CK2 in CFTR: mechanistic aspects of Thr1471 phosphorylation. *PLoS ONE* 8, e74232.

Supporting Figures

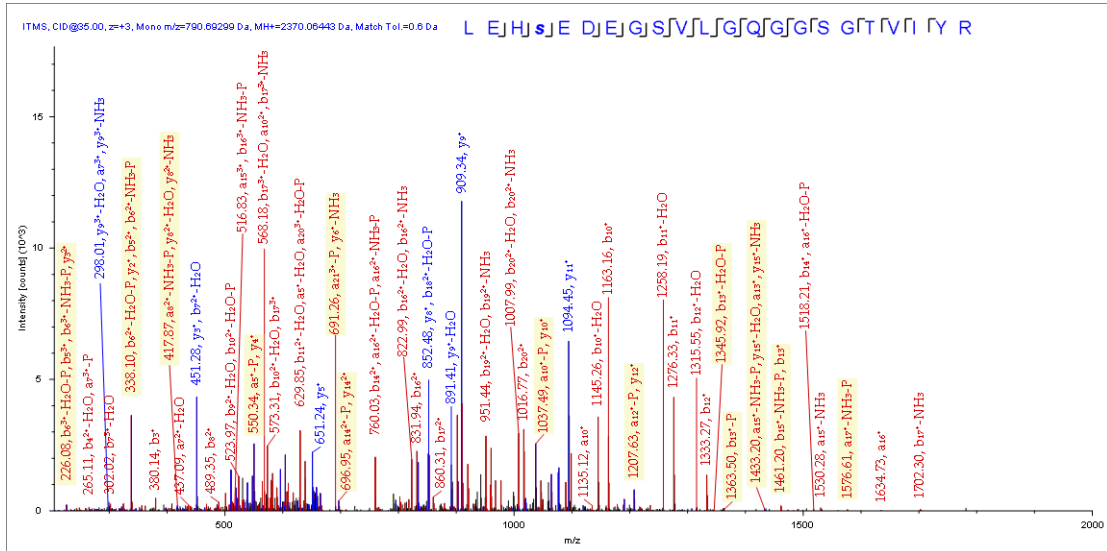
Figure S1



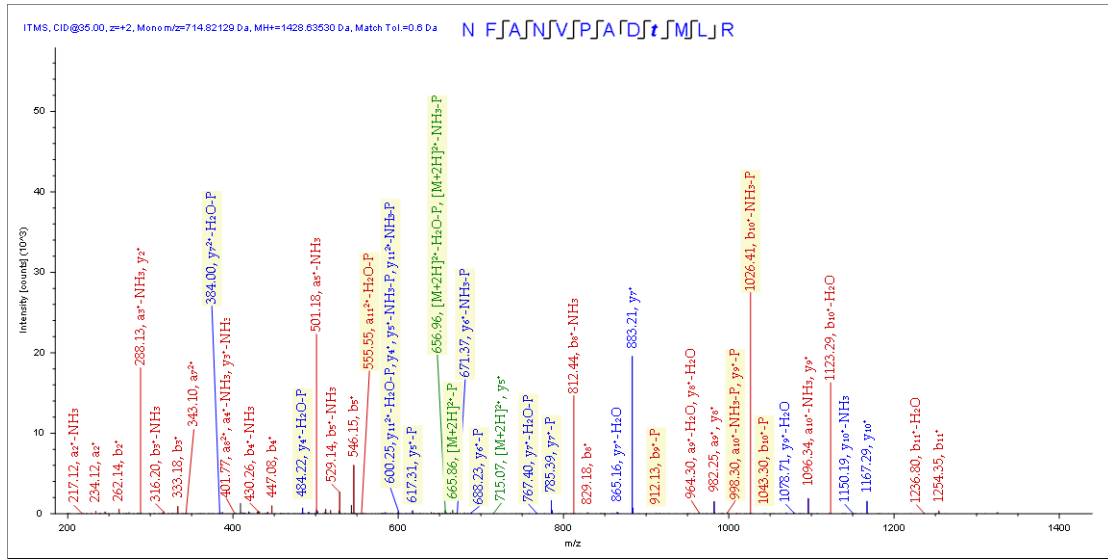
pS1074/pT1075: NRCSpTpFRVK



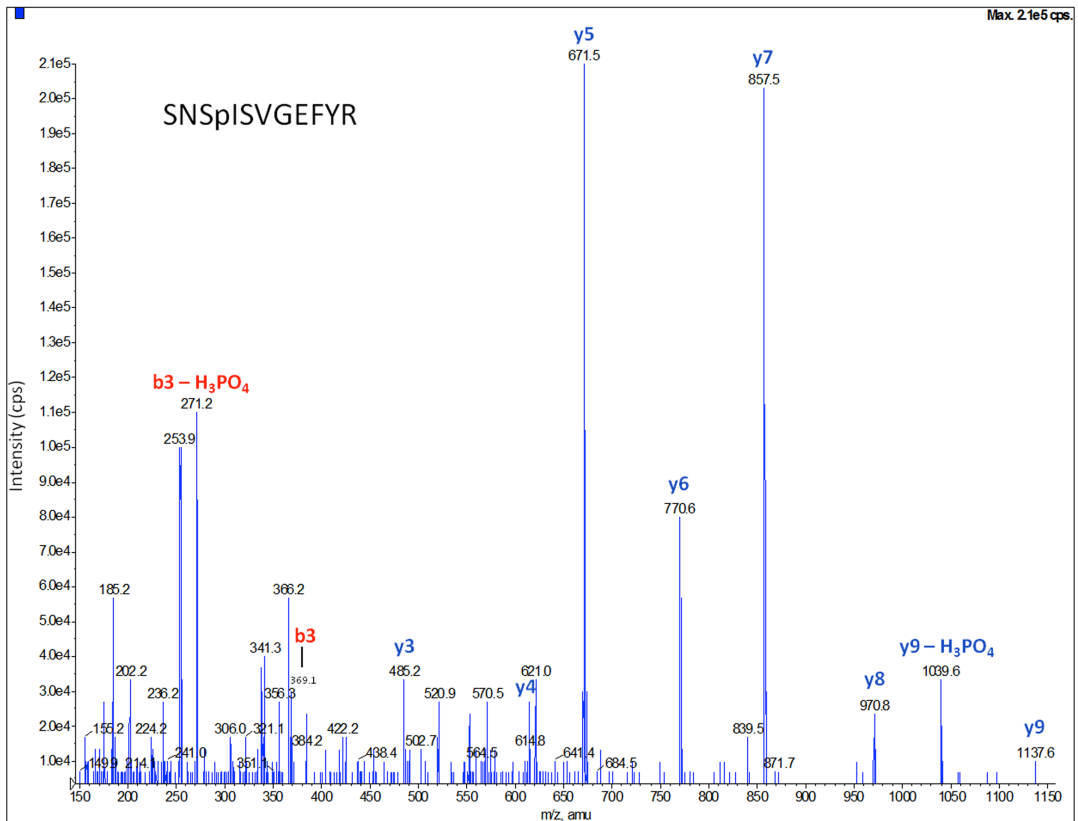
pS1241: LEHSpEDEGSLVGGSGTVIYR



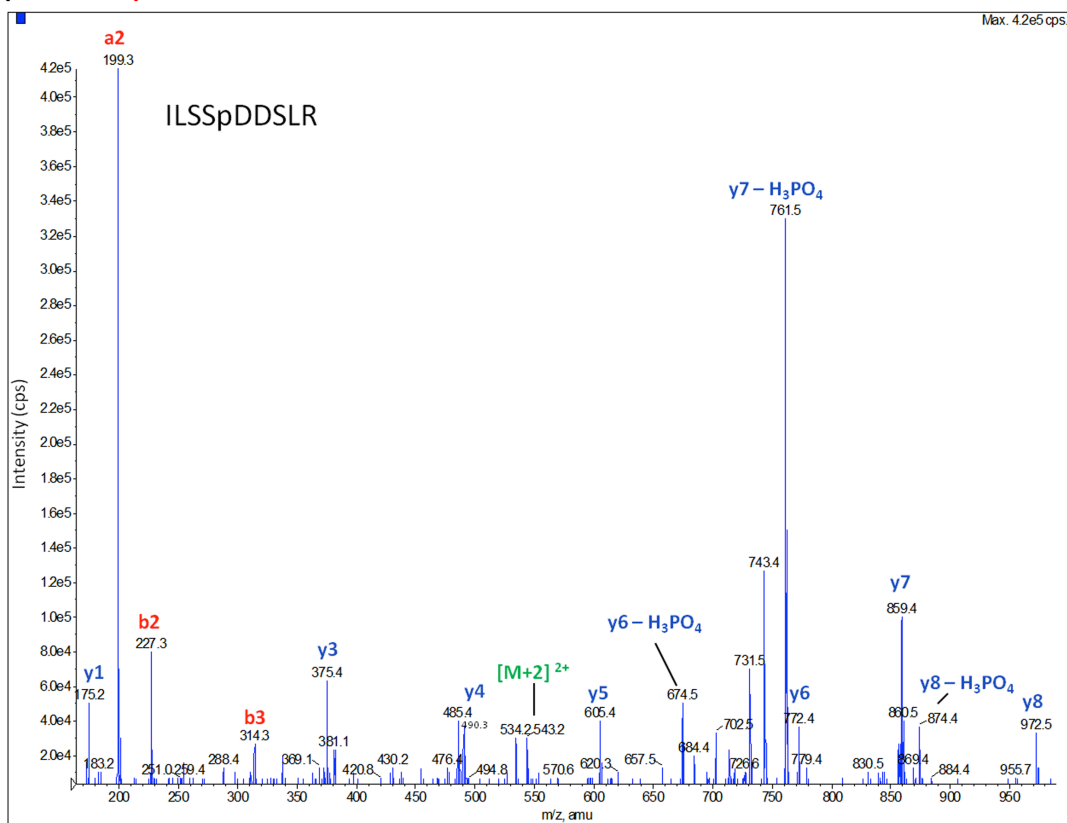
T1287: NFANVPADTPMLR



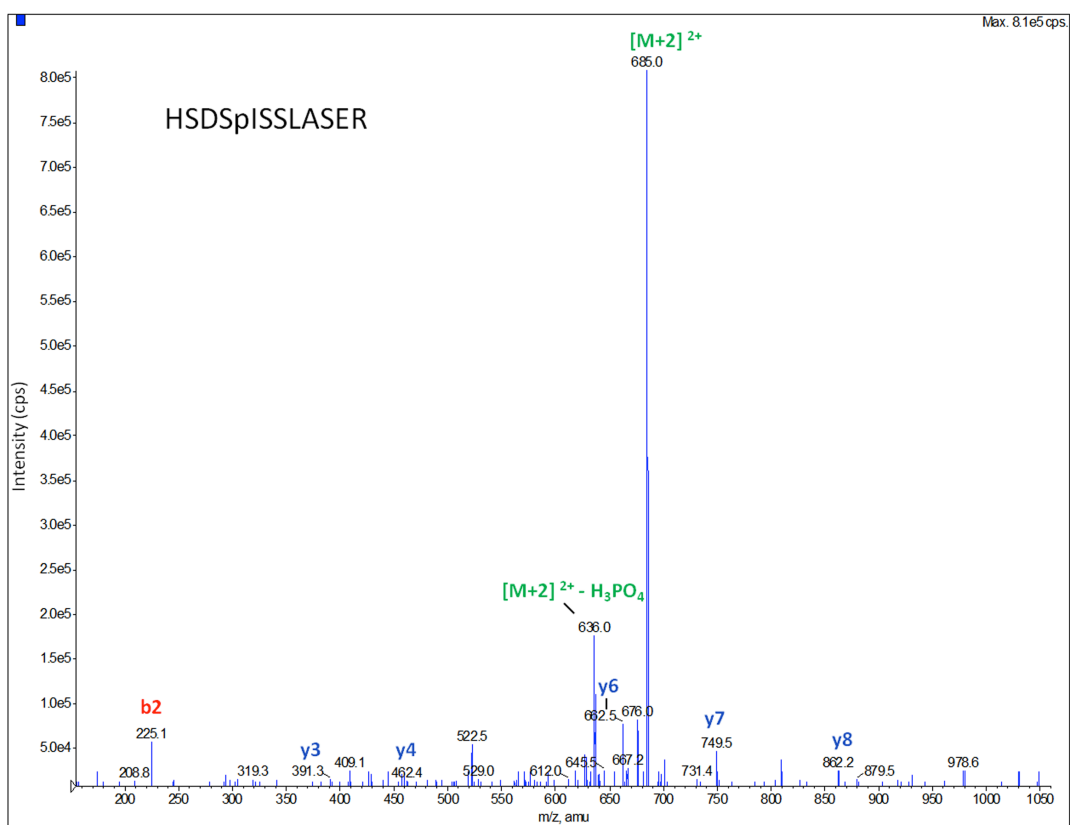
ps910: SNSpISVGEFYR



pS955: ILSSpDDSLR



pS973: HSDSpISLASER



pS1058: MSpCIANLDVSR

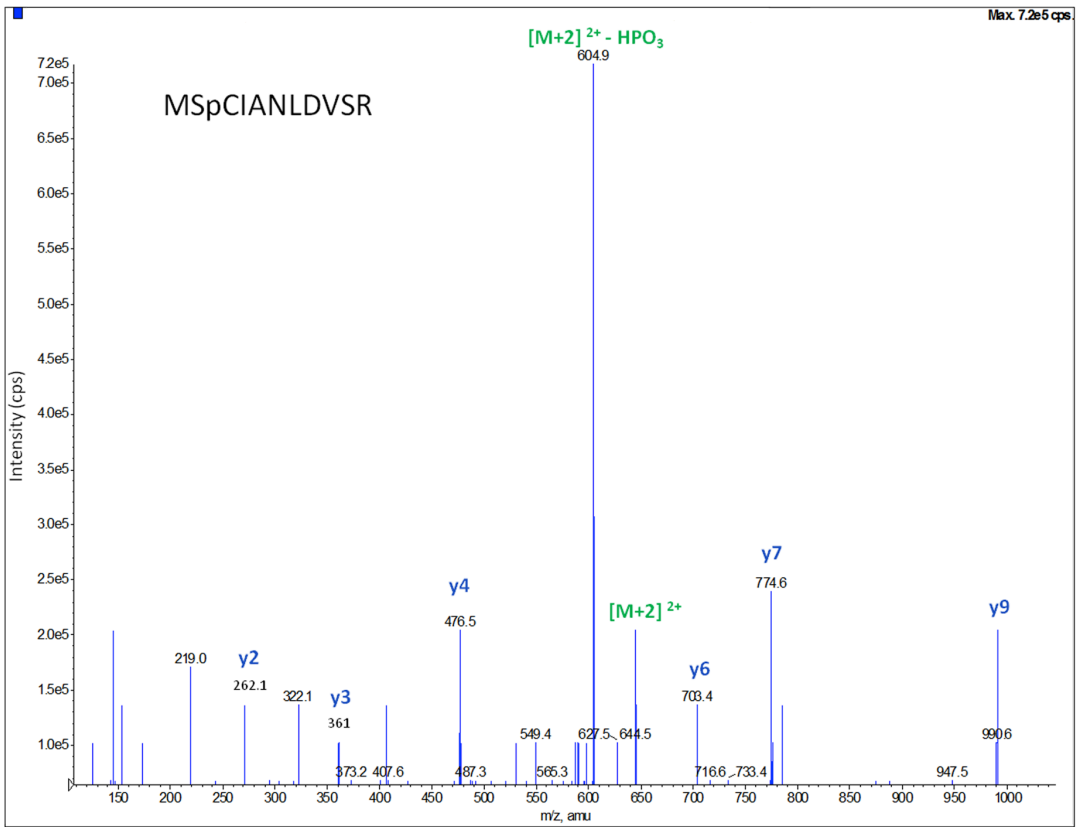
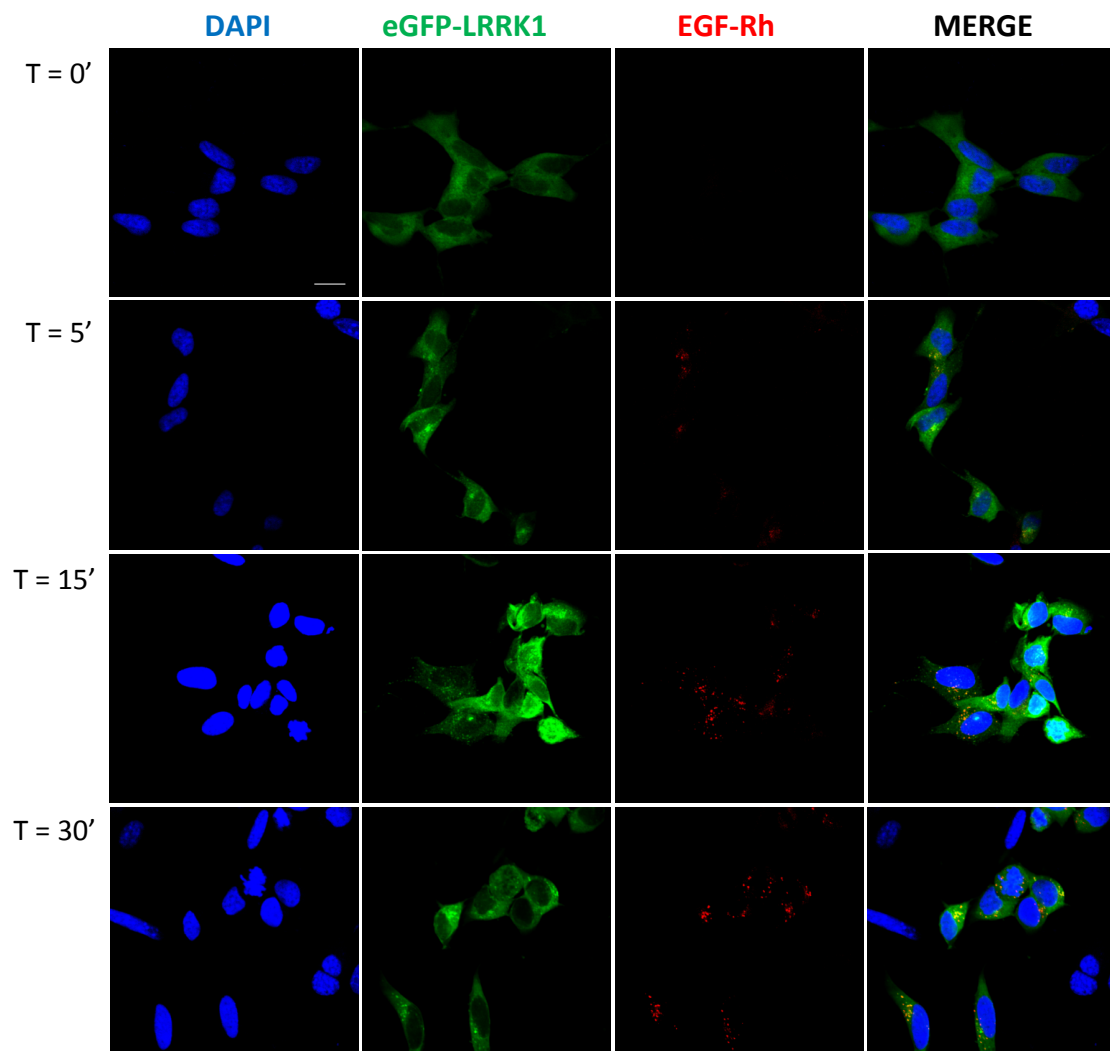


Figure S2

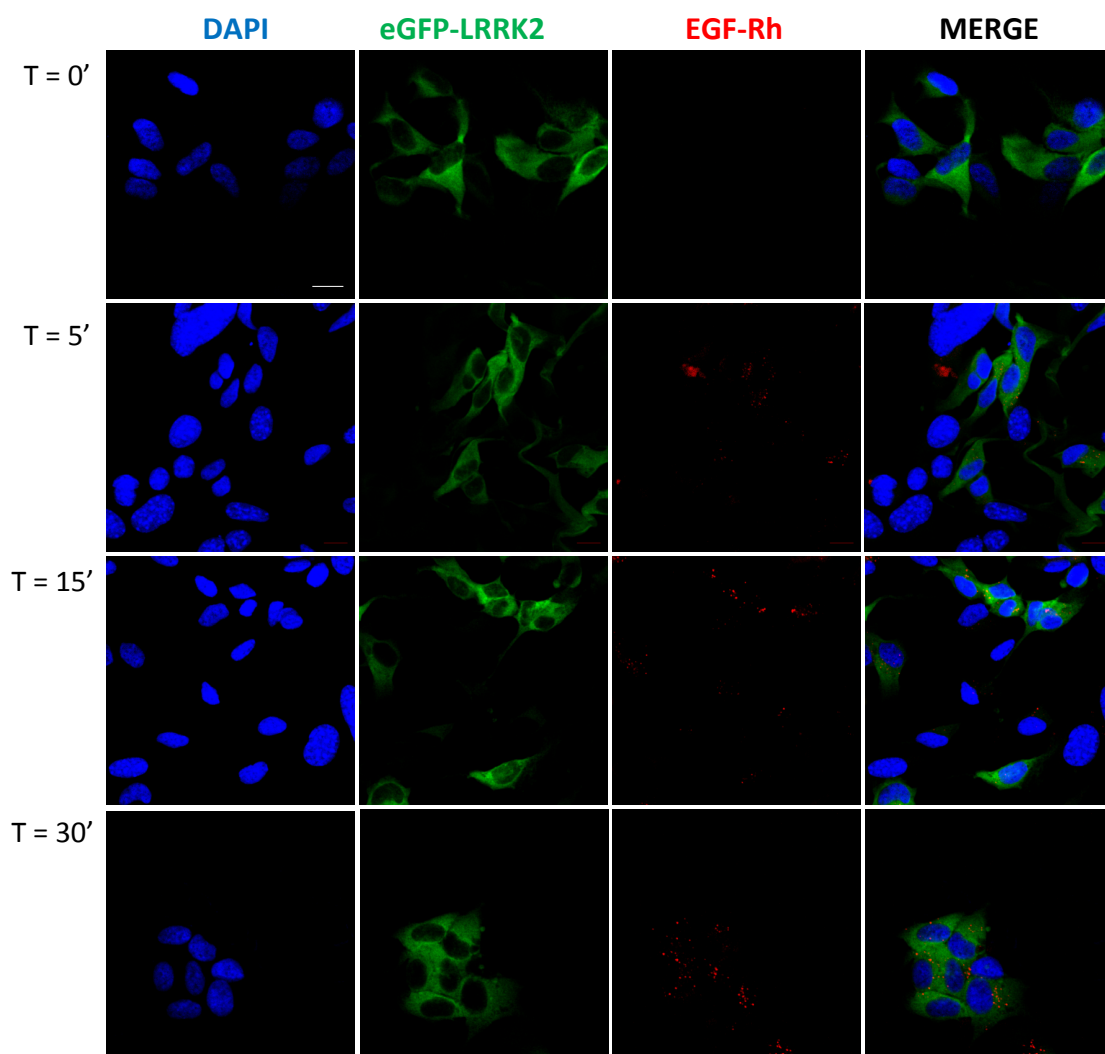
A

SHSY5Y eGFP-LRRK1, ctrl miR



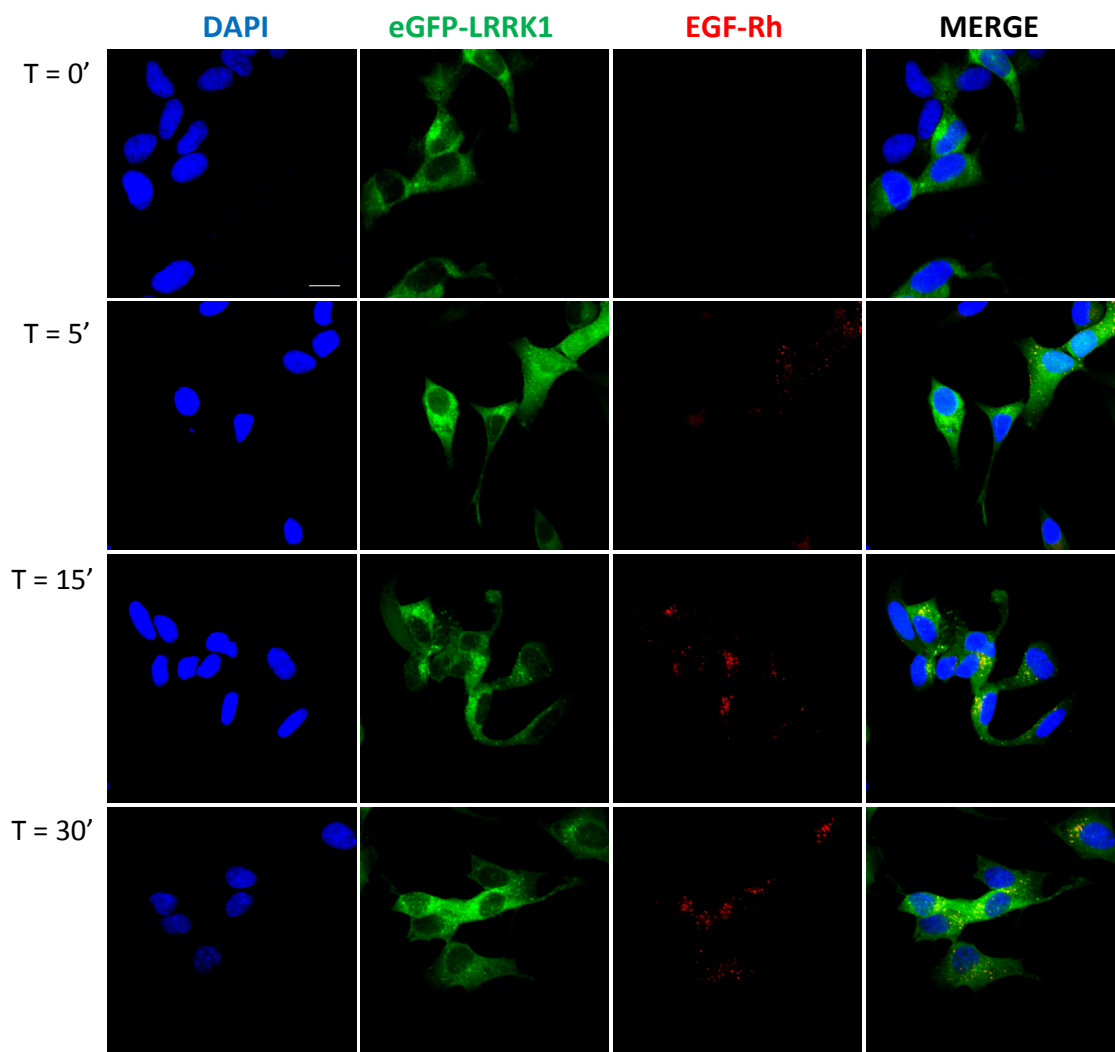
B

SHSY5Y eGFP-LRRK2, ctrl miR



C

SHSY5Y eGFP-LRRK1, LRRK2 RNAi (6251)



D

SHSY5Y eGFP-LRRK2, LRRK1 RNAi (6743)

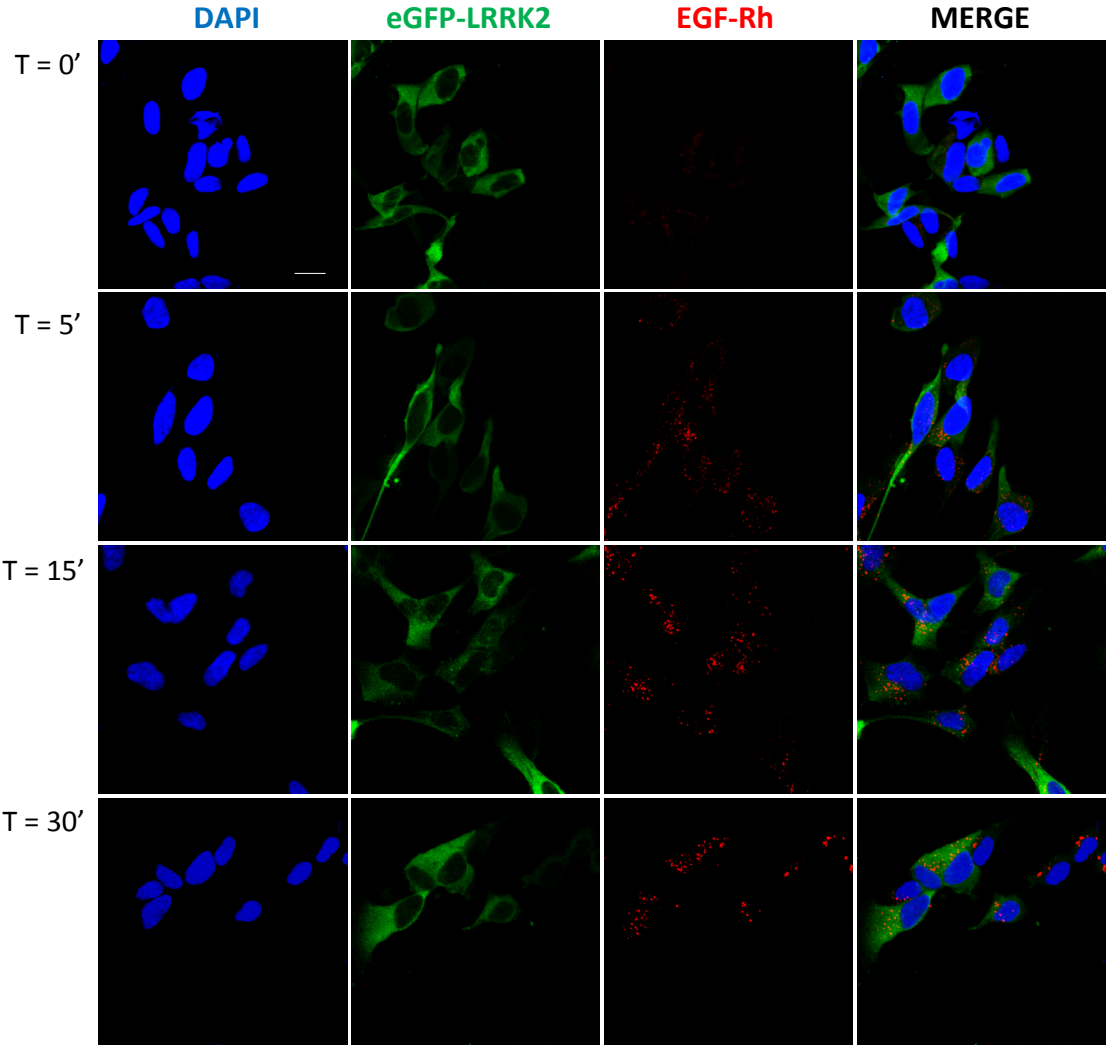


Figure S3

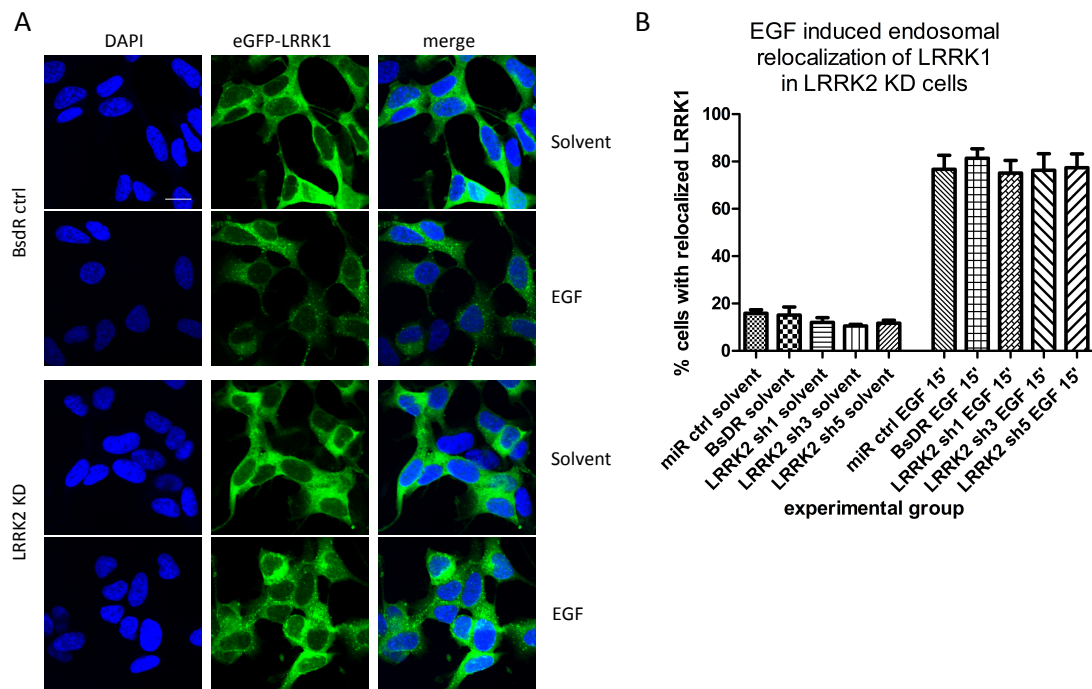


Figure S4

